JAERI－M
5146

# Measurement of the Plasma Current Distribution in a Tokamak Device by α-Particles Injected Transverse to the Toroidal Magnetic Field

(Numerical Calculations of the Particle Orbits and Experimental Arrangement)

February, 1973

S. KAWASAKI*, K. INOUE and T. TAKEDA

日本原子力研究所
Japan Atomic Energy Research Institute

この報告書は，日本原子力研究所が JAERI-M レポートとして，不定期に刊行している研究報告書です．入手，複製などのお問合わせは，日本原子力研究所技術情報部（茨城県那珂郡東海村）あて，お申しこしください．

JAERI-M reports, issued irregularly, describe the results of research works carried out in JAERI. Inquiries about the availability of reports and their reproduction should be addressed to Division of Technical Information, Japan Atomic Energy Research Institute, Tokai-mura, Naka-gun, Ibaraki-ken, Japan.

JAERI-M 5146

# Measurement of the Plasma Current Distribution in a Tokamak Device by $\alpha$-Particles Injected Transverse to the Toroidal Magnetic Field

## ( Numerical Calculations of the Particle Orbits and Experimental Arrangement )

Sunao KAWASAKI*, Kenji INOUE and Tatsuoki TAKEDA

Nuclear Fusion Lab., Tokai, JAERI

( Received February, 1973 )

The report is a continuation of the previous paper in which basic problems in the α-particle probing of a current distribution in the axisymmetric plasma column were elucidated.

In this report, the experimental arrangement for application of the method to the Tokamak device in JAERI ( JFT-2 ) is described. The results of numerical analyses on the α-particle orbits for the resolution of a measured current distribution, the counting rate of the probe particles and the setting errors of the emitter and the detector of α-particle are also described.

---

* Guest Scientist to JAERI.

Permanent Address : Faculty of Science, Kanazawa University, Kanazawa, Japan.

JAERI－M 5146

# アルファ粒子入射によるトカマク型装置のプラズマ電流密度分布測定
## （粒子軌道の数値解析と実験の準備計画）

日本原子力研究所東海研究所核融合研究室

川崎　温*．井上　堅司．竹田　辰興

（1973年2月8日受理）

本報告は，JAERI－memo 4531以後の研究成果のまとめである。実際のJFT－2装置にアルファ粒子入射によるプラズマ電流密度分布測定法を適用するために必要な粒子軌道の数値解析，測定における精度の評価，装置設計に必要なアルファ粒子源，検出器系の検討結果がまとめられている。

* 客員研究員　金沢大学理学部物理学教室

# Measurement of the Plasma Current Distribution in a Tokamak Device by α-Particles Injected Transverse to the Toroidal Magnetic Field

( Numerical Calculations of the Particle Orbits and Experimental Arrangement )

## 1 Introduction

Among many candidates[1] for the techniques to measure the distribution of plasma current which is supposed to be of great importance in the stability character of a Tokamak plasma, probing by a heavy charged particle[2] seems to be one of most promising methods because of the following inherent merits. It is applicable to a closed system such as a Tokamak or a Stellerator and gives no disturbance to the plasma at all. The momentum required for the probe particle is in the moderate range for the reasonable parameters of the containment devices existing now or expected to appear in near future.

In our preceding papers[3)-4)], we showed that α - particles emitted from a radioisotope could be good probe particles in a Tokamak if we injected them into plasma column perpendicularly to the toroidal magnetic field. They are deflected by the Lorentz force $V_r \times B_p$ in the toroidal direction, where $V_r$ is

the radial velocity of the particles and $B_p$ the magnetic field due to plasma current, which is supposed to have only $\theta$ - component. This toroidal drift can be fairly large to be analysed and to give information on the plasma current flowing in the toroidal direction. Using multiple $\alpha$ - beams with various values of parameters such as the energy, injection angle, position of $\alpha$ - source and so on, the distribution of the current could be determined.

This paper discusses some problems relating to the design of the practical arrangements of the measuring system. In section 2, the computer analysis of the particle orbit in the toroidal geometry is given. The effects of the setting of the $\alpha$ - source and the spread in energy and emitted angle of $\alpha$ - particle on the resolution at the detector position is also presented in this section. Section 3 describes the relation between the toroidal drift and the distribution of the plasma current. In section 4, on the basis of the above numerical calculations, the detailed structures of the $\alpha$ - source and detector are presented. A preliminary experiment which is prepared to test these apparatuses in a linear system with a dummy plasma current is also stated in section 5.

## 2 Numerical Analysis of the Orbits of $\alpha$ - Particles

It was shown in ref. ( 3 ) that the $\alpha$ - emitter should be placed in a vacuum a little way off from the plasma boundary in the horizontal plane containing the magnetic axis. When the particle is to be emitted vertically, the momentum of the $\alpha$-particle should be determined so that the path of the $\alpha$ - particle may cross the magnetic axis which coincides with the center of the

plasma column in case of a cylindrical plasma ( Fig. 1 ). This was called " the standard orbit " in ref. ( 3 ). For the parameters of JFT - 2 the calculated standard orbit is shown in Fig. 2. It does not close itself due to the toroidal effect, neverthless, it should be noted that the validity of the discussion stated before still holds even in such a fat torus as JFT - 2. The position of the detector or detector array is assumed as shown in Fig. 2. It should be movable on a plane crossed by the particle orbit. The following factors are supposed to cause the errors in the analysis of the plasma current distribution.

1 ) Error of the $\alpha$ - particle energy from the prescribed one. ( $\Delta E/E$ )

2 ) Error in the setting of the emission angle from the vertical plane containing the emitter and the toroidal axis. $\Delta\theta_{tor}$

3 ) Error in the setting of the emission angle in the vertical plane containing the emitter and the toroidal axis. $\Delta\theta_{pol}$

4 ) Misalignment of $\alpha$ - source in radial direction. $\Delta R$ ( Displacement of the plasma column in the opposite direction ).

5 ) Misalignment of $\alpha$ - source in vertical direction. $\Delta Z$

The effects due to the above factors on the toroidal drift at the detector position shown in Fig. 2 are evaluated with the electronic computer of JAERI, FACOM - 230/60.

The parameters of JFT - 2 used here are summarized in Table 1. In the calculation, the plasma current distribution and

the safety factor at the plasma boundary ( $q_a$ ) are assumed to be homogeneous and 2, respectively. The results are given in Figs. 3 a) - e). The relative errors in the toroidal drift S ( $\Delta S/S$ % ) are summarized in the following way.

a ) $\frac{\Delta E}{E}$ ( Fig. 3a ).

$$\frac{\Delta S}{S} \simeq 0.25 \frac{\Delta E}{E}$$

where $\frac{\Delta S}{S}$ is given in percent. The limit of $\frac{\Delta E}{E}$ is about 8 % for the value of $\frac{\Delta S}{S}$ of 2 %.

b ) $\Delta\theta_{pol}$ ( Fig. 3b ).

$$\frac{\Delta S}{S} \simeq 0.9\ \Delta\theta_{pol}\ ,$$

where $\Delta\theta_{pol}$ is given in degree. The current distribution is obtained by measuring the toroidal drift for various values of the parameters of the $\alpha$ - beam, e.g. of the emission angle in the vertical plane $\theta_{pol}$. In this case $\theta_{pol}$ varies from 90° to about 0°. ( See Fig. 11 ). The maximum $\Delta\theta$pol allowable for 2 % of $\frac{\Delta S}{S}$ is 2.2°, which is quite small compared with the range of variation of $\theta_{pol}$.

c ) $\Delta\theta_{tor}$ ( Fig. 3c )

$$\frac{\Delta S}{S} \simeq 32\ \Delta\theta_{tor}\ ,$$

where $\Delta\theta_{tor}$ is given in degree. It is evident that $\Delta\theta_{tor}$ causes the most serious error in the resolution of the plasma current distribution. The magnetic field of the Tokamak has little focusing character in the toroidal direction and the deviation of the emission angle from the vertical plane

$\Delta\theta_{tor}$ produce directly a serious ambiguity in the measurement of the toroidal drift. Therefore this error must be minimized with the use of a narrow slit at the sacrifice of a considerable decrease in the beam intensity. For $\frac{\Delta S}{S}$ = 2 %, $\Delta\theta_{tor}$ should be very small to be 0.0625°. The problem of the slit system is treated in section 4.

d ) $\Delta R$ ( Fig. 3d ).

$$\frac{\Delta S}{S} \simeq 8.5\ \Delta R,$$

where $\Delta R$ is in cm. It is concluded from the above equation that 0.24 cm of the error in the radial direction causes 2 % of $\frac{\Delta S}{S}$. In practice the $\alpha$ - source can be set in the device in the accuracy within ±1 mm. $\Delta R$, however, is also concerned with the displacement of the plasma column. Therefore an auxiliary method may be necessary to determine its position against the plasma column.

e ) $\Delta Z$ ( Fig. 3e )

$$\frac{\Delta S}{S} \simeq 2.2\ \Delta Z,$$

where $\Delta Z$ is in cm. Compared with the effect of $\Delta R$, it seems to be less important.

## 3 Toroidal drift and the distribution of the plasma current

In this section the results of the calculated toroidal drift as a function of the energy of $\alpha$ - particles for various distributions of the plasma current are described. An $\alpha$ - particle is assumed to be emitted vertically. The parameters of JFT - 2 in this calculation are listed in Table 2.

Avoiding the use of the complex actual magnetic field, we simulate it by modifying the field strength for a case of a cylindrical plasma imbeded in a longitudinal magnetic field[3] as

$$B_z = B_{zo} \frac{R_o}{R_o + r\cos\theta}$$

and

$$B_p = B_{po} \frac{R_o}{R_o + r\cos\theta} \qquad \text{( See Fig. 4 )}$$

The radial component $B_r$ and the externally applied vertical field $B_v$ are estimated to be several tens gauss and neglected ( Appendix I ). The equations of motion of $\alpha$ - particle are with the same notations in ref. ( 3 ),

$$\ddot{r} = r\dot{\theta}^2 + \frac{e}{m}[\, r\dot{\theta}B_z - \dot{z}B_\theta \,]$$

$$\ddot{z} = \frac{e}{m}[\, \dot{r}B_\theta - r\dot{\theta}B_r \,]$$

and

$$\ddot{\theta} = -\frac{2\dot{r}}{r}\dot{\theta} + \frac{1}{r}\frac{e}{m}[\, \dot{z}B_r - \dot{r}B_z \,]$$

Substituting into these equations the following expressions and writing them in non-dimensional form,

$$B = 0$$

$$B_z = B_{zo} \frac{R_o}{R_o + r\cos\theta}$$

and

$$B_p = B_\theta = \mu_o \frac{J_o}{2a^n} r^{n+1} \frac{R_o}{R_o + r\cos\theta} \qquad \text{( case N )}$$

or

$$B_p = B_\theta = \mu_o \frac{p+2}{p} J_o\left[\frac{r}{2} - \frac{r^{p+1}}{a^p(p+2)}\right] \frac{R_o}{R_o + r\cos\theta}$$

( case P )

where the cases N and P correspond with the monotonously radially increasing and decreasing distributions of the plasma current, respectively. ( See Figs. 2 and 3 in ref. (3) ).

For the case N, the equations of motion are reduced as,

$$\ddot{r} = r\dot{\theta}^2 + \frac{1}{1 + r\cos\theta}\left[ r\dot{\theta} - B\frac{r^{n+1}}{a^{n+1}}\dot{z} \right]$$

$$\ddot{z} = \dot{r}\frac{1}{1 + r\cos\theta} B \frac{r^{n+1}}{a^{n+1}}$$

$$\ddot{\theta} = -\frac{2\dot{r}\dot{\phi}}{r} - \frac{\dot{r}}{r}\frac{1}{1 + r\cos\theta}$$

and for the case P,

$$\ddot{r} = r\dot{\theta}^2 + \frac{1}{1 + r\cos\theta}\left[ r\dot{\theta} - B\frac{p+2}{pa}\left\{r - \frac{2r^{p+1}}{a^p(p+2)}\right\}\dot{z} \right]$$

$$\ddot{z} = \dot{r}\frac{1}{1 + r\cos\theta} B\frac{p+2}{pa}\left[ r - \frac{2r^{p+1}}{a^p(p+2)} \right]$$

$$\ddot{\theta} = \frac{2\dot{r}\dot{\theta}}{r} - \frac{r}{r}\frac{1}{1 + r\cos\theta} \quad ,$$

where r, z and a are normalized by $R_o$ and t is by $\frac{m}{eB_z} = t_o$. B is a measure of $B_p$ and is given by

$$B = \frac{\frac{I}{2\pi a}\mu_o}{B_{zo}}$$

For solving these equations, Runge-Kutta-Gill method is used. Initial values given in the input data are listed in the Appendix II with the symbols used in the program. The whole computer program are also given in the Appendix.

In the following, the indexes of the shape of the current distribution, P and N are represented by MP and MN for convenience of the description of the computer results.
At first we calculated the temporal evolution of the azimuthal angle $\theta$ for various initial azimuthal velocity $\dot{\theta}$. The results are shown in Figs. 5 and 6 for MN and MP = 1. For the large value of $-\dot{\theta}$ ( $-\dot{\theta} > 0.45$ ), $\theta$ does not oscillate, but decreases monotonously. In other words the orbits of $\alpha$ - particle with large initial $-\dot{\theta}$ link the magnetic axis. The orbit of the particle with the initial $\dot{\theta} = -0.45$ corresponds to the standard orbit. The toroidal drift are calculated as functions of time in the cases of various distribution and shown in Fig. 7. The toroidal drifts after one complete Larmor cycle are summarized in Fig. 8. This result coincides with the rough estimations in ref. ( 3 ) very well. For a hybrid form of the current distribution of the two cases, only a little modification is necessary and the drift is easily calculated, and the examples of the result are shown in Figs. 9 and 10.

From these figures it is concluded that the distribution of the plasma current can be determined with good accuracy for certain classes of the current distribution.

## 4 The design of $\alpha$ - source

We decided that the most favourable $\alpha$ - source is $^{210}Po$. It could be treated and completed as a practical $\alpha$ - source in the Radioisotope Production Development Section of JAERI. There are some remaining problems to be decided in $\alpha$ - source.

a ) Energy spread by self - absorption

$^{210}Po$ of 10 mC has $6.4 \times 10^{15}$ atoms and emits $3.8 \times 10^{8}$ $\alpha$ - particles per sec. The total weight is about $2.24 \times 10^{-6}$ g and the volume $2.4 \times 10^{-7}$ cm$^3$. The surface area of $\alpha$ - source is estimated to be about 4 mm$^2$ and the depth should be of the order of 700 Å. The energy spread $\Delta_o$ caused by $\alpha$'s passage through the source itself can be evaluated by Symon's formula[6] as

$$\Delta_o = \frac{2cm_e x c_o^2}{\beta^2} b$$

where $c = 0.150 \frac{Z}{A}$ g$^{-1}$ cm$^2$, $c_o$ is the light velocity and b is about 0.35 from the graph of ref. ( 6 ). For our $\alpha$ - source $\Delta_o$ is estimated as

$$\Delta_o \simeq 6 \times 10^{-4} \text{ Mev}$$

This can be negligible, considering that the 8 % of $\frac{\Delta E}{E}$ is still allowable in our criterion of designing the source.

b ) Energy spread by absorption foil

As stated before the energy of $\alpha$ is about 1 Mev when the toroidal magnetic field is $1 \times 10^4$ gauss. $\alpha$ - particle from $^{210}Po$ have the energy of 5.3 Mev and it must be reduced to 1 Mev by passing through the absorber foil. If we choose Au or Ni as the absorber material, the energy decrease in the foils are obtained by the well - known Bethe's formula as

$$\left( \frac{dE}{dx} \right)_{Ni} = 177 \text{ Kev/}\mu\text{m}$$

$$\left( \frac{dE}{dx} \right)_{Au} = 202 \text{ Kev/}\mu\text{m}.$$

The foil thickness required for the energy decrease of 4.3 Mev are determined as

$$d = 24.3 \ \mu\text{m} \qquad \text{for Ni}$$

and

$$d = 21.3\ \mu m \qquad \text{for Au.}$$

The energy struggling appears also in these foils. The energy after passing through the foil has a distribution of the approximately Gaussian shape and its half-value width is

$$\left( \frac{\Delta}{E} \right) \simeq 4.0\ \% \qquad \text{for Ni}$$

and

$$\left( \frac{\Delta}{E} \right) \simeq 5.1\ \% \qquad \text{for Au.}$$

These spread are both permissible in view of the resolution analysis.

c ) Slit system in front of the source

With the distance $\ell$ between the exit slit and the source ( see below ) the effective solid angle is $\frac{d_1 d_2}{\ell^2}$.

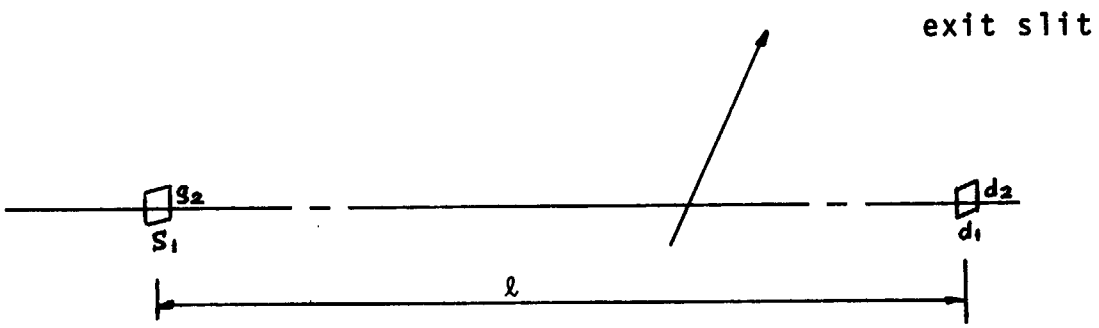


By using the relation between the drifts and the errors of initial conditions for the homogeneous current distribution, the dimension of the image of the source in the toroidal direction is given as

$$\frac{\Delta S}{S} \simeq 32\ \frac{\frac{1}{2}( s_1 + d_1 )}{\ell} \times 57.3 \qquad ( \text{in } \% ).$$

A choice of $s_1$ and $d_1$ as

$$s_1 \simeq 0.3 \text{ mm}$$

and

$$d_1 \simeq 0.25 \text{ mm}$$

gives about 5 % of the error in the toroidal drift, taking $\ell$ to be 100 mm. In this case the solid angle $\Delta\Omega$ is

$$\Delta\Omega \sim 0.5 \times 10^{-4} \text{ steradian for } d_2 = 2 \text{ mm}.$$

The counting rate at the detector's position will be about $3.0 \times 10^3$/sec if we use 10 mC of the source. The width of the image will be largely broadened in the toroidal direction to be ±5 mm. A Si surface barrier detector in common use, however, has a sufficient surface area and can detect the - beam. Use of focusing system to reduce the beam spread in front of the source is possible in principle, but seems difficult in practice. ( See Appendix III ).

d ) Setting system

α - source is set in the horizontal plane and in the meridional plane passing the center of the box of measurement. It should be able to be rotated within the range of ± 5° in the toroidal direction and from 0° to 90° in the poloidal direction.

The detector is on the surface of the cylinder with the radius of 120 cm and is movable vertically and in toroidal direction. Besides them, it can be tilted in the poloidal direction from about 30° to - 30° on the spot. The schematic figure of the positions of the α - source and the detector is shown in Fig. 11. Examples of the design of the α - source and the detector

assembly are shown in Figs. 12 and 13.

e ) Detector

The solid state detector of Si surface barrier type may be the best for the detection of the 1 Mev α - beam. Use of a detector array consisting of several detectors in a line will be convenient in the measurement of the plasma current and in its calibration. " Nuclear Triode ", a solid state detector of a position and energy spectrometer type produced by Nuclear Diodes Inc. may also be useful except that it is expensive.

## 5 Preliminary experiment

To test the α - source and detector system, a small-sized preliminary experiment is being planned. Instead of the plasma current, a dummy current flowing in a conducting rod will produce $B_\theta$. No toroidal field is applied. The overall view of the experimental arrangement is shown in Fig. 14. The vacuum chamber is composed of the Dow-Corning Pyrex tubes " double tough " of 15 cm diameter. The total length of the device is about 100 cm. The α - source is set on one end and the particle is emitted nearly along the axis of the device. About 40 cm apart from the source a rod of 15 mm diameter crosses the axis and 10 kA of the pulsed current flows in it. The α - beam is deflected by the magnetic field produced by the pulsed current and the deviation x is estimated to be in this geometry

$$x = 0.12 \times 10^{-5} I \quad ( \text{in m} )$$

when I is the current flowing in the rod and it is measured in Ampere. For I = 10 kA, this gives $x \simeq 1.2$ cm. The current will be supplied by the discharge of a bank of electrolytic condensers ( 500 V and 10 μF ). The preliminary experiment is now prepared.

## Acknowledgement

The authors are grateful to Mr. T. Tazima for the help during the numerical calculations.

## References

1 ) There are many techniques proposed to measure the magnetic field in plasma cloumn, related to the propagation and the reflection of laser light, for example:

C. B. Weeler and J. Troughton: Plasma Physics 11 541 (1969).

C. Etiévant and I. Fidone: Plasma Physics 12 985 (1970).

M. Murakami and J. F. Clarke: Nucl. Fusion 11 147 (1971).

F. W. Perkins: Princeton University Report MATT 818 (1970).

D. E. Evans and P. G. Carolan: Phys. Rev. Lett. 25 1605 (1970).

L. Kellerer: Proceedings of the 4th European Conf. on Controlled Fusion and Plasma Physics (C.N.E.N. Rome 1970) p 125.

Microwave technique may also be useful.

R. Cano, I. Fidone and M. J. Schwartz: Phys. Rev. Lett. 27 783 (1971).

R. Cano, I. Fidone, G. Chaignot and M. J. Schwartz: Phys. Fluids 15 1635 (1972).

2 ) A few proposals to measure the magnetic fields in plasma column by an energetic beam probe are presented:

F. C. Jobes and R. L. Hickok: Nucl. Fusion 10 195 (1970).

They, however, put the stress on the possibility of measuring the space potential and the fluctuation in the plasma. We have another private communication from T. Tamano on this problem.

3 ) s. Kawasaki, K. Inoue, T. Takeda and M. Yoshikawa: JAERI-memo 4596 ( Sept. 1971 ).

4 ) S. Kawasaki and K. Inoue: Nucl. Fusion 12 387 (1972).

5 ) S. Itoh et al: JAERI-memo 4084 ( July, 1970 ).

6 ) B. Rossi: High energy Particles, Prentice Hall, N. Y. 1952.

## Appendixes

### I Effect of the vertical magnetic field $B_v$ applied externally on the toroidal drift

$B_v$ is estimated to be 0 — 80 gauss in JFT - 2. The toroidal field $B_t$ is about $1.5 \times 10^4$ gauss and the poloidal one is $0.8 \times 10^3$ gauss at the plasma surface. Therefore the effects of $B_p$ and $B_v$ on the orbit of $\alpha$ - particles can be treated small perturbations which are independent on each other.

The Lagrange function of a charged particle in the toroidal geometry is

$$L = \frac{1}{2} m \left( r^2 + ( r\dot{\theta} )^2 + z^2 \right) + \left( \dot{r}A_r + r\dot{\theta}A_\theta + \dot{z}A_z \right)$$

We easily obtain

$$\theta = \frac{e}{m} \int_0^t \frac{( A_{\theta_0} r_0 - A_\theta r )}{r^2} dt + \theta_0$$

$B_v$ produces only the toroidal drift. With a similar treatment as in ref. ( 3 ), the azimuthal drift caused by $B_v$ is about twice of the following expression,

$$\theta \simeq \frac{1}{m} \int_0^{\pi/(\frac{eB}{m})^{1/2}} \frac{c ( r_{max}^2 - r^2 )}{r^2} dt$$

$$\simeq \frac{1}{m} \int_0^{\pi/(\frac{eB}{m})^{1/2}} \frac{c2RA ( 1 - \cos \frac{eB}{m} t )}{R} dt$$

$$\simeq \frac{2Ac}{m} \frac{\pi}{\frac{eB}{m}} \frac{1}{R}$$

at maximum, where R is the Larmor radius of $\alpha$ - orbit and the vector potential $A_\theta$ is taken as

$$A = cr.$$

$B_v$ is given by

$$B_v = \text{rot } A \,|_z = 2c.$$

The toroidal drift by $B_v$ is

$$2R\theta \sim A \frac{eB_v}{m} \frac{\pi m}{eB_t} \sim 0.7 \text{ cm}$$

with the parameters of JFT - 2. This is about one-tenth of the drift caused by the plasma current. It may be easy to detect the drift by $B_v$ and to cancel out experimentally.

## II Computer program for calculating the orbits

| Input data | Symbols in the program |
|---|---|
| $a = \frac{25\ (cm)}{90\ (cm)} = 0.27778$ | AI |
| $B = \frac{4\pi\times10^{-7}\times250\times10^{3}\ (A)}{2\times25\times\pi\,(cm)\times1.5\times10^{4}(gauss)} = 0.13333$ | BI |
| $r = \frac{25}{90} = 0.27778$ | Y(1) |
| $\dot{r} = 0$ | Y(2) |
| $z = 0$ | Y(3) |
| $\dot{z} = 0$ | Y(4) |
| $\theta = 0$ | Y(5) |
| $\dot{\theta} = -0.50$ | Y(6) |
| Step in Runge Kutta Method = 0.01 | H |
| N = 0, 1, 2, 3 | MN |
| P = 1, 2, 3, 4 | MP |

Program

```
C       ARKK
C       ALPHA RYUSHI NO KIDO KEISAN, RUNGE
C       KUTTA GILL HO, LINEAR GEOMETRY
C       WITH MODIFICATIONS.
C       INJECTION PERPENDICULAR HO
C       CURRENT DISTRIBUTION INCREASING
C       CONTINUOUSLY WITH RADIUS.
        DIMENSION A(6), B(4), C(4), Q(6), Y(6),
      1           Z(6), T(6), R(6)
```

```
    1 FORMAT ( 9F8.5,I2 )
   10 READ ( 5,1 ) AI, BI, ( Y(N), N=1,6 ), H, MN
      X = 0.0
      L = 1
      WRITE ( 6, 2000 )
 1000 DO 100 I = 1,6
  100 Q(I) = 0.0
      PX = X
      A(1) = 0.0
      A(2) = 0.5*H
      A(3) = A(2)
      A(4) = H
      A(5) = H
      A(6) = A(2)
      B(1) = 1.0
      B(2) = 0.2928932
      B(3) = 1.707107
      B(4) = 1.0/3.0
      C(1) = 0.0
      C(2) = 0.7071068*H
      C(3) = - C(2)
      C(4) = 0.0
C
      DO 200 J = 1,4
      X = PX + A(J)
      CALL DIFEQ( Z, Y, AI, BI, MN )
      DO 200 K = 1, 6, 1
      T(K) = A( J+2 )*Z(K) - Q(K)
      R(K) = B(J)*T(K)
```

```
      Y(K)=Y(K)+R(K)
      Q(K)=3.0*R(K)-T(K)+C(J)*Z(K)
  200 CONTINUE
      TI=L*H
      L=L+1
C
 2000 FORMAT(1HO,9X,4HTIME,7X,6HRADIAL,5X,8HTOROIDAL,4X
     19HAZIMUTHAL)
C
      WRITE(6,3000)TI,(Y(K),K=1,5,2)
C
 3000 FORMAT(1HO,3X,F10.4,3E13.5)
C
      IF(1.2-L*H)4000,4000,1000
      CONTINUE
C
 4000 STOP
      END
      SUBROUTINE DIFEQ(Z,Y,AI,BI,MN)
      DIMENSION Z(6),Y(6)
      Z(1)=Y(2)
      Z(2)=Y(1)*(Y(6)**2)+(Y(1)*Y(6)-BI*Y(4)*EXP((MN+1)*
     1ALOG(Y(1)/AI)/(1.0+Y(1)*COS(Y(5)))
      Z(3)=Y(4)
      Z(4)=Y(2)*BI*EXP((MN+1)*ALOG(Y(1)/AI)/(1.0+Y(1)*
     1COS(Y(5)))
      Z(5)=Y(6)
      Z(6)=-2.0*Y(2)*Y(6).Y(1)-Y(2)/Y(1)*(1.0+Y(1)*COS(Y(5)))
      RETURN
      END
```

## III Focusing system of the α - beam

It may reduce the toroidal spread in the α - beam to put a focusing system in front of the source. The large mass and momentum prevents the α - particle from being deflected to a great amount. For exsample, let us consider the two-dimensional focusing system represented by a conformal mapping

$$W = K \sin \frac{\pi}{\ell} z.$$

Putting

$$W = U + iV$$

$$z = x + iy$$

where U, V, x and y are real values, the contour lines

$$U = K \sin\frac{\pi}{\ell} x \cosh\frac{\pi}{\ell} y = \text{const}$$

give the potential figure shown below.

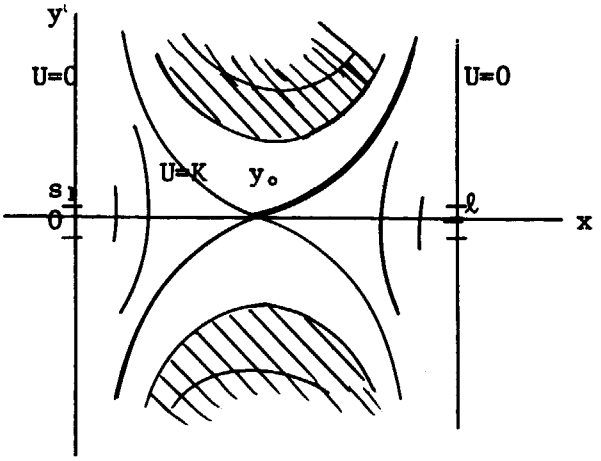


If we replace the hatched region by the conductor electrodes and put them in the potential $U_0$,

$$U = K \cosh\frac{\pi}{\ell} y_0$$

and

$$E_y = -\frac{\partial U}{\partial y} = -\frac{U_o}{\cosh\frac{\pi}{\ell} y_o} \sin\frac{\pi}{\ell} x \cdot \frac{\pi}{\ell} \sinh\frac{\pi}{\ell} y$$

The equation of motion in y-direction for a charged particle entering from the slit $S_1$ in x-direction is

$$\frac{d^2y}{dx^2} = -\frac{eU_o}{2E_o \cosh\frac{\pi}{\ell} y_o} \frac{\pi}{\ell} \sin\frac{\pi}{\ell} x \cdot \sinh\frac{\pi}{\ell} y,$$

where $E_o$ is the energy of the particle and the approximation

$$E_o >> U_o$$

is used. Taking $y = \ell y'$, $x = \ell x'$ and assuming $y' << 1$, we get

$$\frac{d^2y'}{dx'^2} = -K'\pi \sin\pi x' \cdot y', \quad \text{where} \quad K' = \frac{eU_o}{2E_o \cosh\frac{\pi}{\ell} y_o} \pi \ .$$

This is a kind of Mathiew's equation. We put

$$y' = C_o + C_1 x' + (K'\pi)S.$$

By the perturbation method we obtain the following expression.

$$S = \frac{C_o}{\pi^2} \sin\pi x' + \frac{C_1}{\pi^2} \sin\pi x' \cdot x' + \frac{2C_1}{\pi^3} \cos\pi x'.$$

From this solution the focal length f of the system is calculated to be

$$f \simeq \frac{1}{2K'} = \frac{E_o \cosh\frac{\pi}{\ell} y_o}{eU_o \pi}$$

or in our case for $y_o$ = 3 mm, $\ell$ = 10 mm and $U_o$ = 10 kV,

$$f \simeq 50 \text{ cm}.$$

This value of f is clearly too large. With above analysis, we concluded that such a beam focusing system is not imposible to apply, but quite difficult.

Table 1

| | | |
|---|---|---|
| Major radius of the magnetic axis | $R_o$ | 90 cm |
| Plasma radius | a | 25 cm |
| Energy of α - particle | E | 1.0 Mev |
| Toroidal magnetic field | $B_t$ | 1.0 Wb/m$^2$ |
| Safety factor | $q_a$ | 2.0 |
| Position of α - source | R | 130 cm |
| | Z | 0 cm |

Table 2

| | | |
|---|---|---|
| Toroidal magnetic field | $B_t$ | 1.5 Wb/m$^2$ |
| Plasma current ( total ) | I | 250 kA |
| Position of α - source | R | 115 cm |
| | Z | 0 cm |

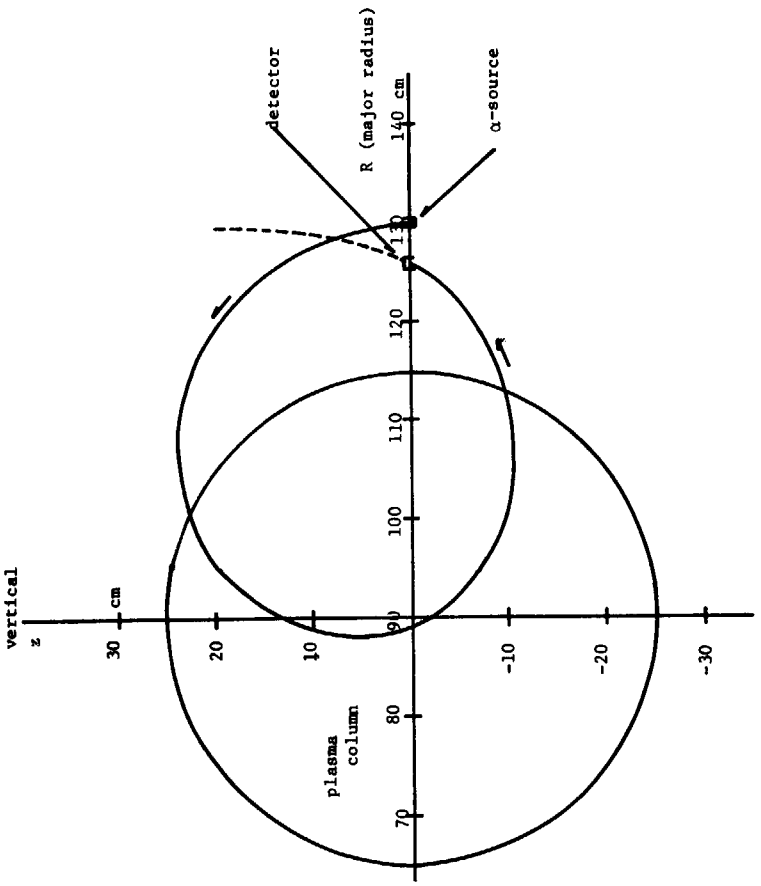


Fig. 2 The standard orbit calculated for JFT - 2.
A vertical displacement due to the toroidal curvature can be seen.
The detector is assumed to be set in a horizontal plane for convenience of the calculation.

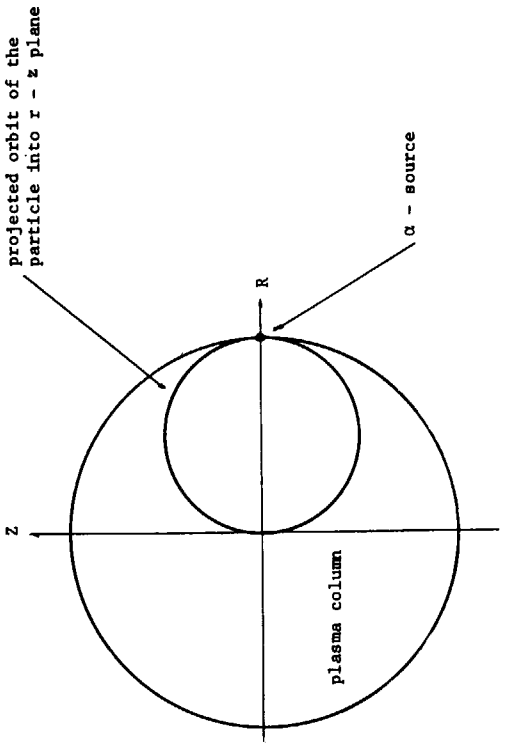


Fig. 1 Standard particle orbit. The external magnetic field $B_t$ is perpendicular to the paper from the surface to the back.

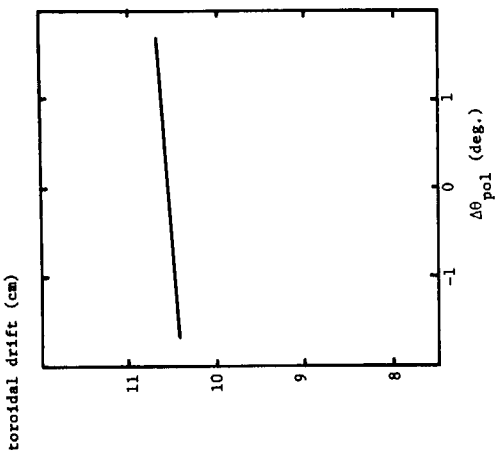


Fig. 3(a) Toroidal drift as a function of $\Delta E/E$. (%).




Fig. 3(b) Toroidal drift as a function of $\Delta\theta_{pol}$ (deg.).

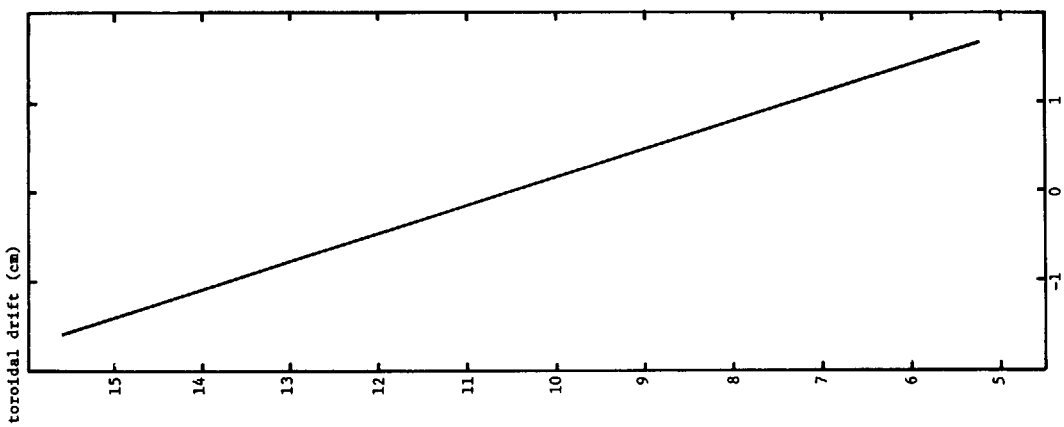


Fig. 3(c) Toroidal drift as a function of $\Delta\theta_{tor}$.

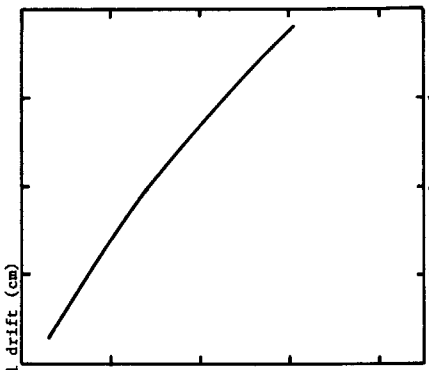


Fig. 3(d) Toroidal drift as a function of $\Delta R$

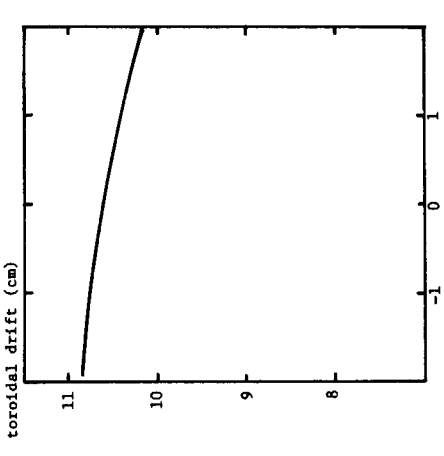


Fig. 3(e) Toroidal drift as a function of $\Delta Z$

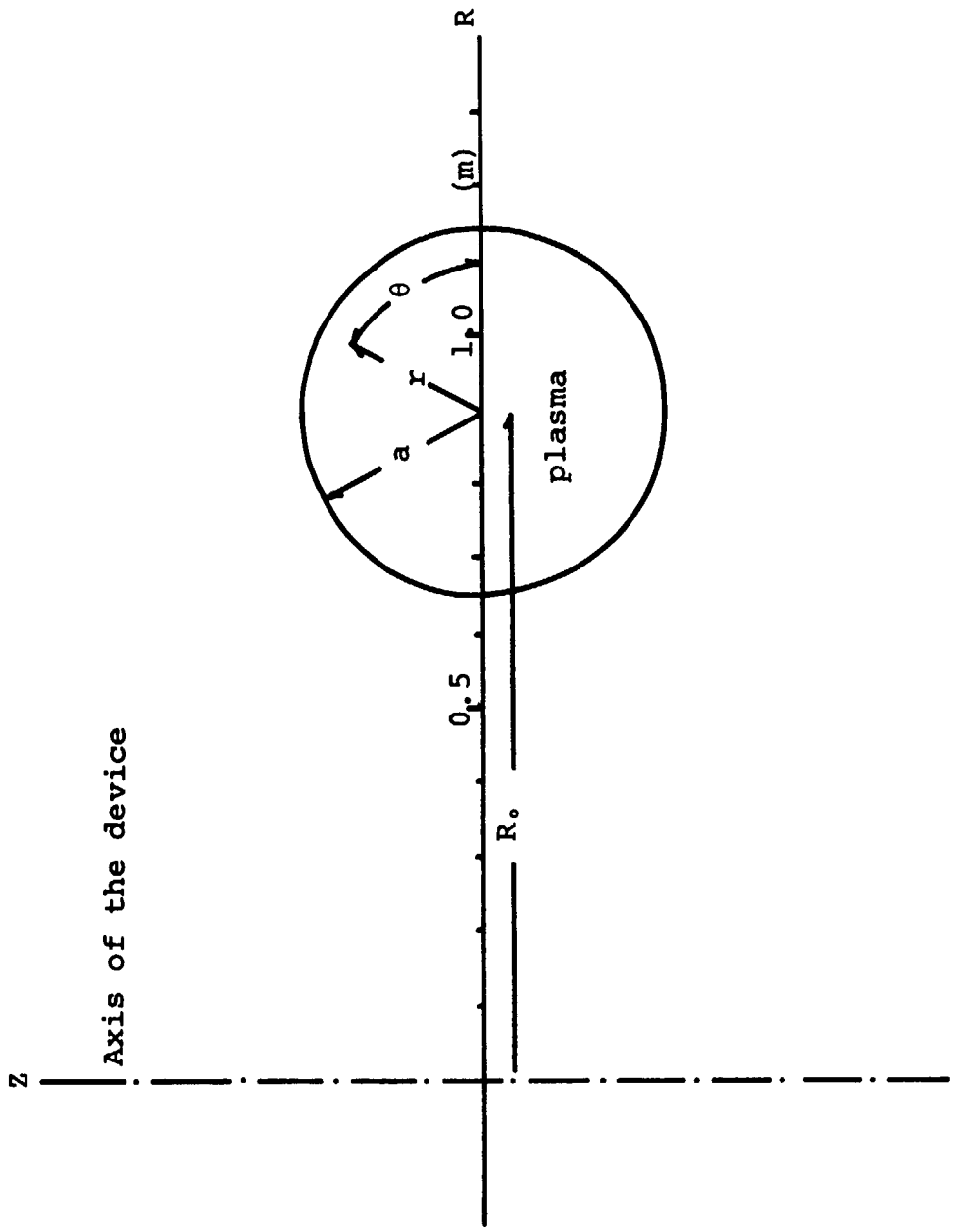


Fig. 4 Toroidal co-ordinates, frequently this is called " pseudo - toroidal " co-ordinates.

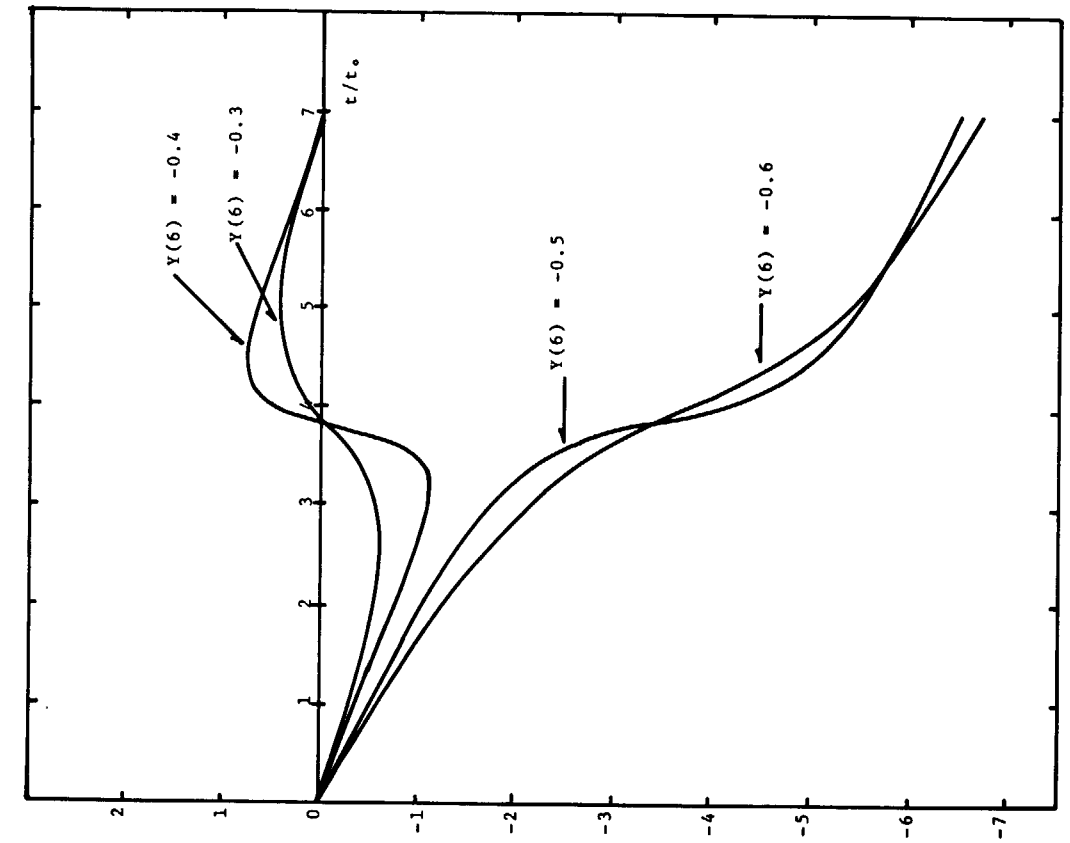


Fig. 6 Time evolution of the azimuthal co-ordinate of the α - particle for MP = 1.

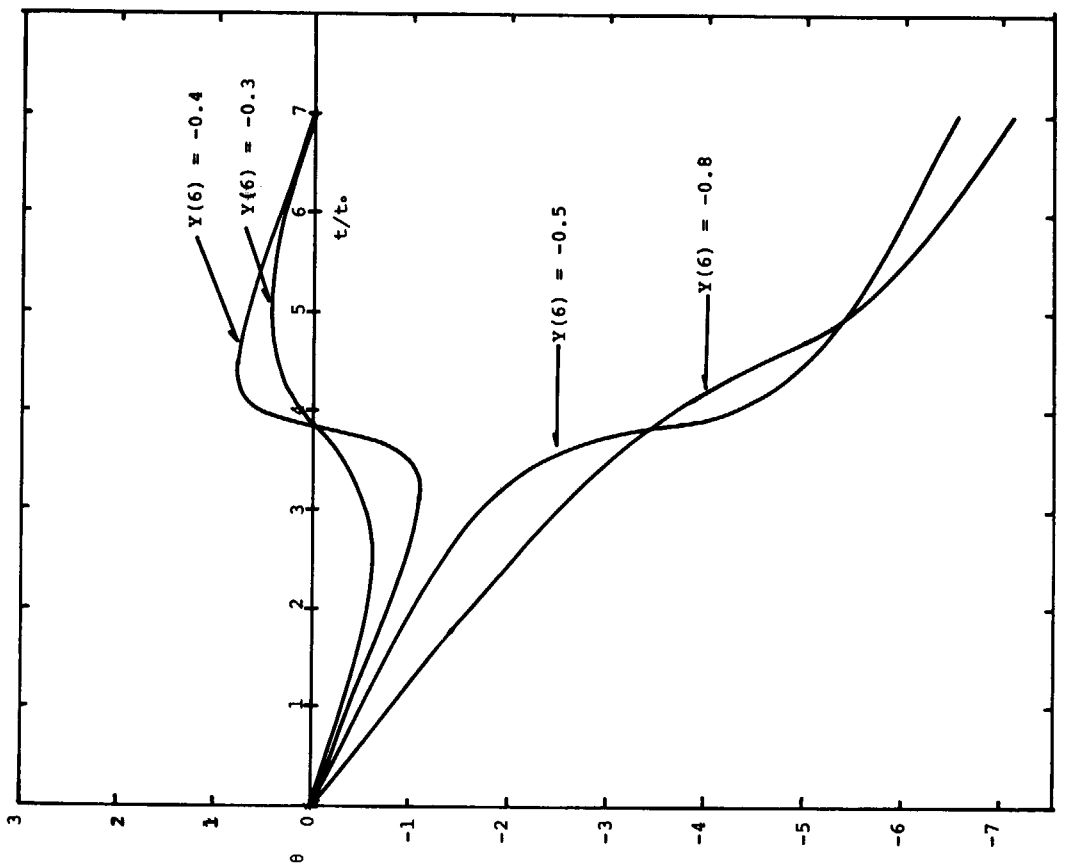


Fig. 5 Time evolution of the azimuthal co-ordinate of the α - particle for MN = 1

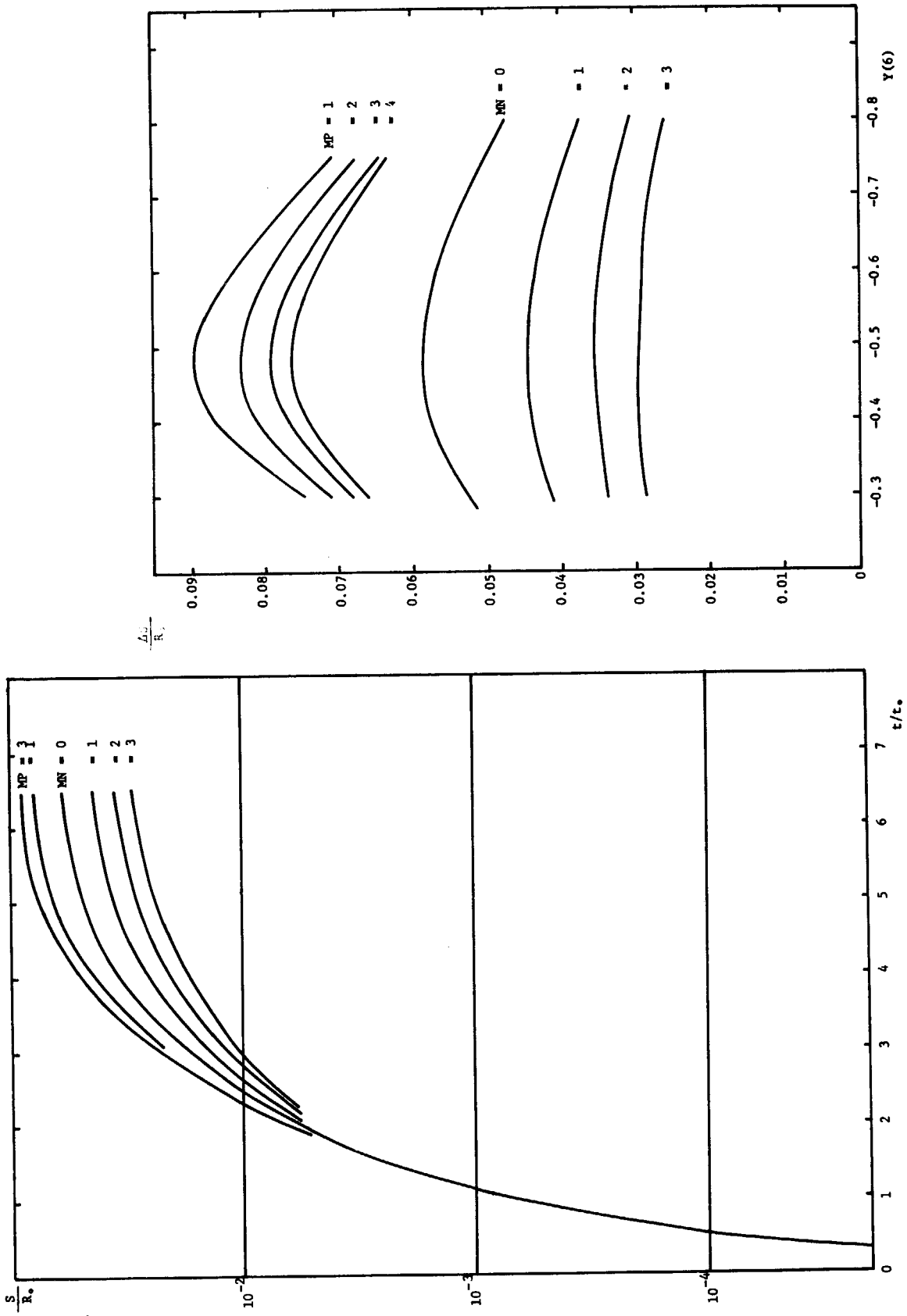


Fig. 7 Toroidal drifts as functions of t for various distributions.




Fig. 8 Toroidal drifts for various distributions of the plasma current.

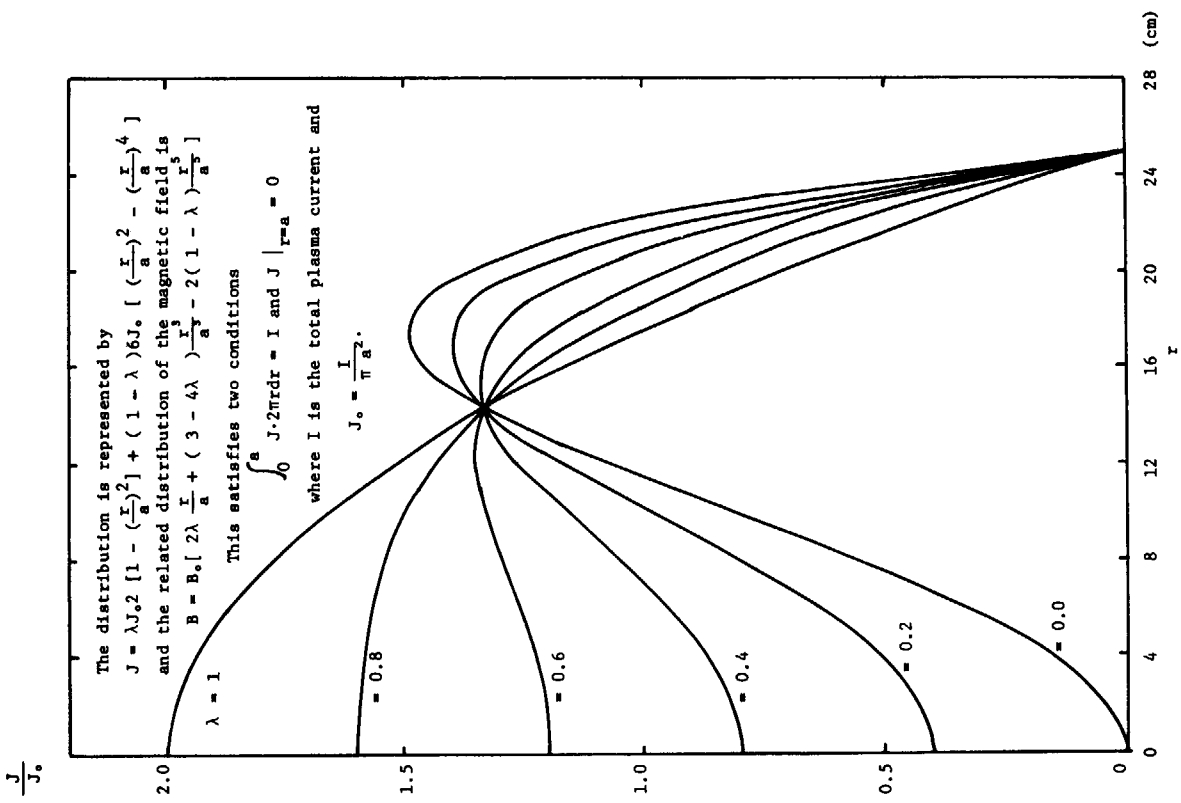


Fig. 9 Current distributions in a hybrid form.

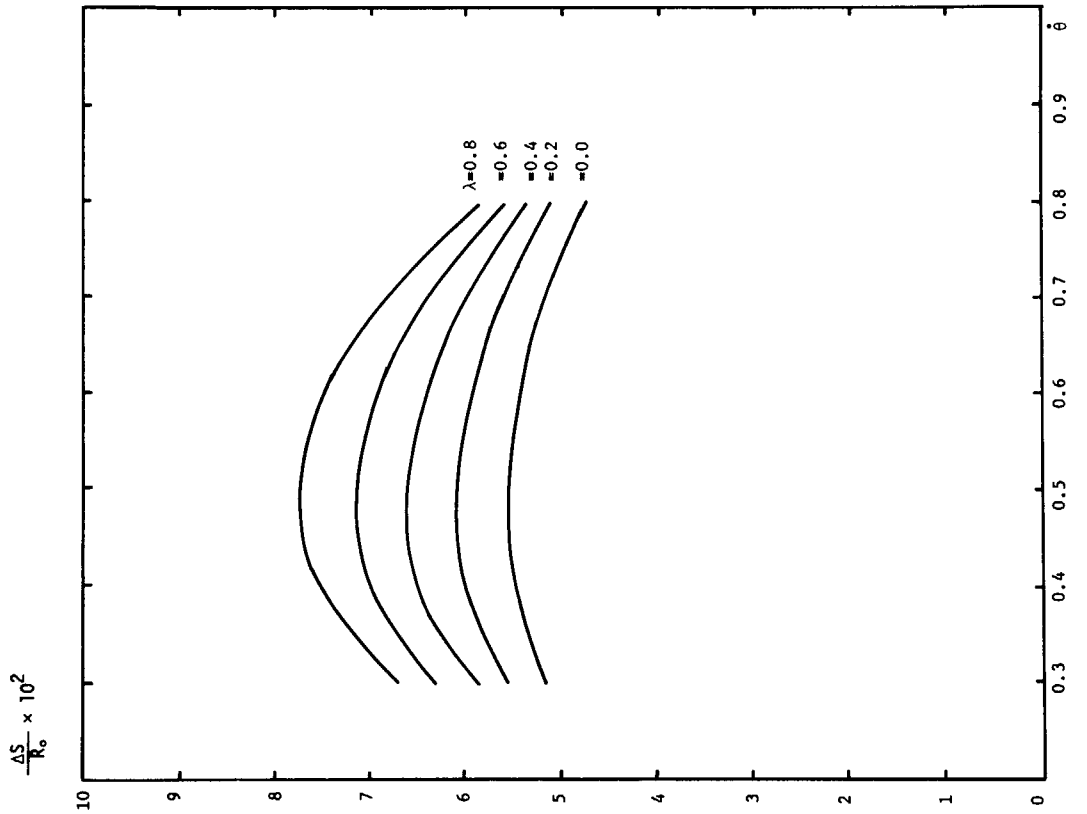


Fig. 10 Toroidal drifts for hybrid distributions of the plasma current

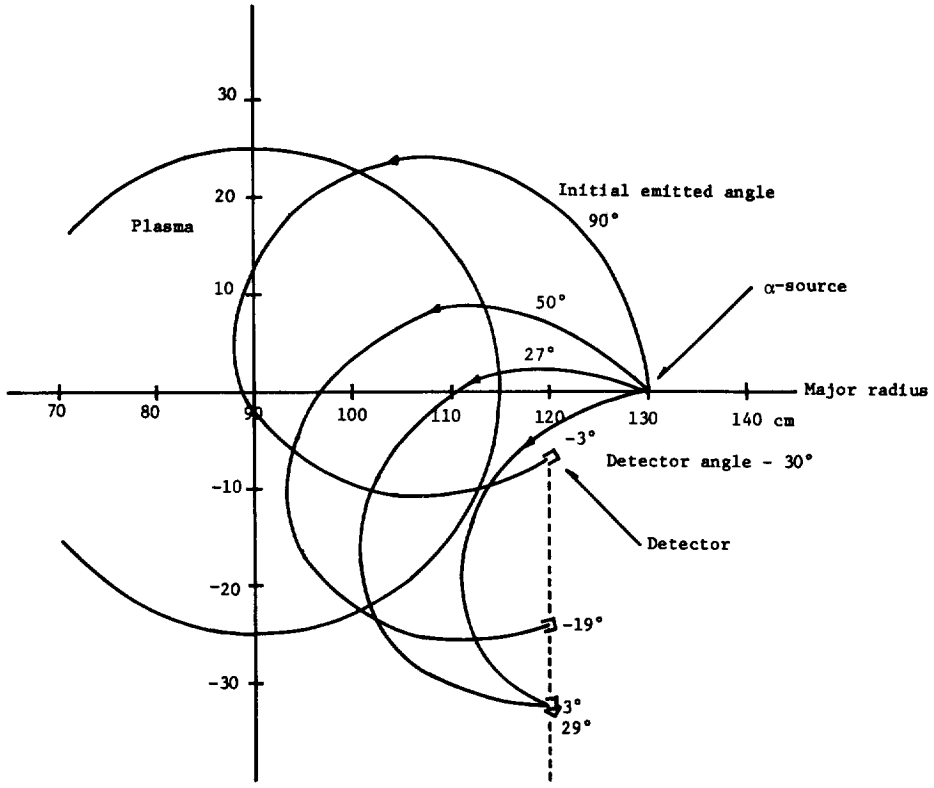


Fig. 11 Schematic Figure of the α - source and the detector positions for various α - orbits.

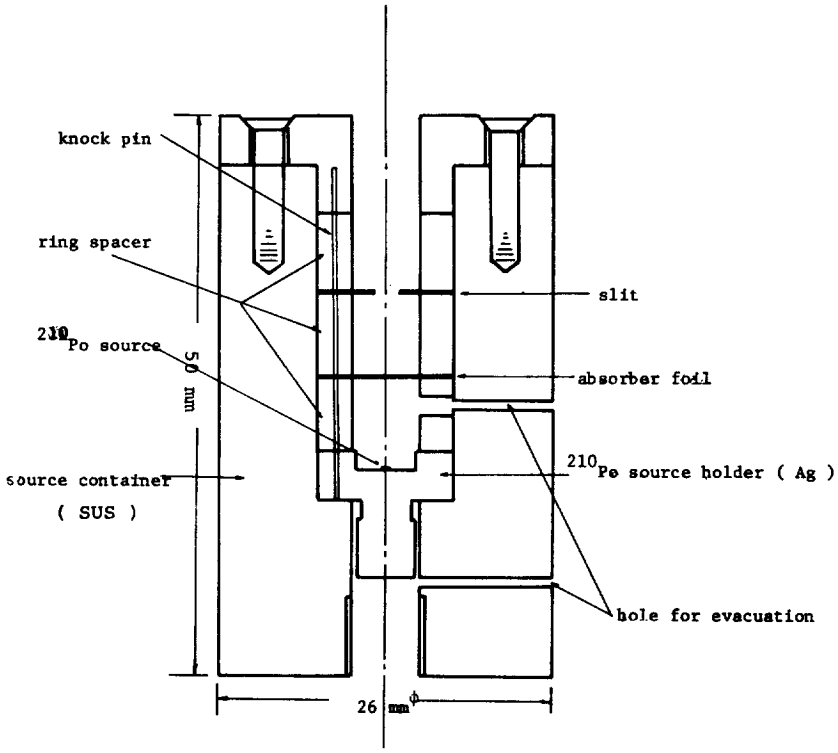


Fig. 12 $^{210}Po$ source assembly. This assembly is mounted on the movable holder.

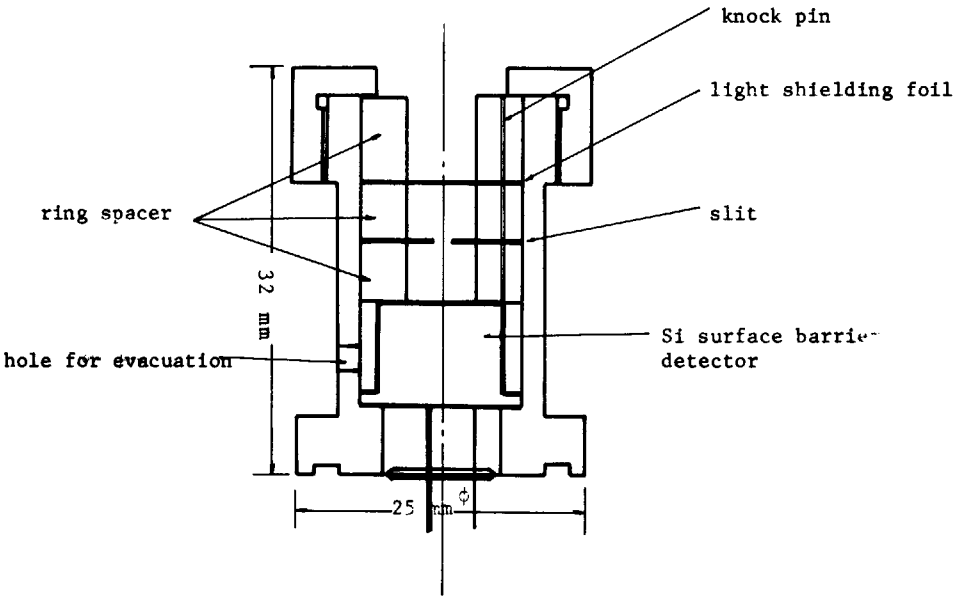


Fig. 13 Detector assembly. This assembly is mounted on the movable holder.

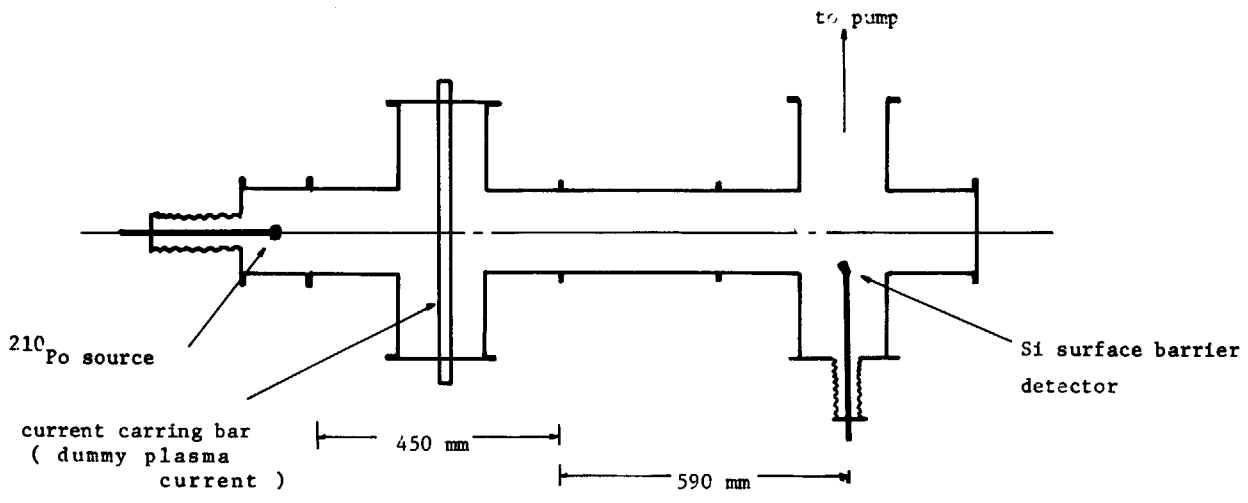


Fig. 14 Schematic arrangement of the preliminary experiment.